Combined inhibition of JAK2-STAT3 and SMO-GLI1/tGLI1 pathways suppresses breast cancer stem cells, tumor growth, and metastasis

Daniel Doheny[1,*], **Sherona Sirkisoon**[1,*], **Richard L. Carpenter**[1,#], **Noah Reeve Aguayo**[1], **Angelina T. Regua**[1], **Marlyn Anguelov**[1], **Sara G. Manore**[1], **Austin Arrigo**[1], **Sara Abu Jalboush**[1], **Grace L. Wong**[1], **Yang Yu**[1], **Calvin J. Wagner**[1], **Michael Chan**[2,3], **Jimmy Ruiz**[2,4], **Alexandra Thomas**[2,4], **Roy Strowd**[2,5], **Jiayuh Lin**[6], **Hui-Wen Lo**[1,2]

[1]Department of Cancer Biology, Wake Forest University School of Medicine, Winston-Salem, NC

[2]Wake Forest Comprehensive Cancer Center, Wake Forest University School of Medicine, Winston-Salem, NC

[3]Department of Radiation Oncology, Wake Forest University School of Medicine, Winston-Salem, NC

[4]Department of Hematology and Oncology, Wake Forest University School of Medicine, Winston-Salem, NC

[5]Department of Neurology, Wake Forest University School of Medicine, Winston-Salem, NC

[6]Department of Biochemistry and Molecular Biology, University of Maryland School of Medicine, Baltimore, MD

Abstract

Triple-negative breast cancer (TNBC) and HER2-positive breast cancer are particularly aggressive and associated with unfavorable prognosis. TNBC lacks effective treatments. HER2-positive tumors have treatment options but often acquire resistance to HER2-targeted therapy after initial response. To address these challenges, we determined whether novel combinations of JAK2-STAT3 and SMO-GLI1/tGLI1 inhibitors synergistically target TNBC and HER2 breast cancer since these two pathways are concurrently activated in both tumor types and enriched in metastatic tumors. Herein, we show that novel combinations of JAK2 inhibitors (ruxolitinib and pacritinib) with SMO inhibitors (vismodegib and sonidegib) synergistically inhibited *in vitro* growth of TNBC and HER2-positive trastuzumab-resistant BT474-TtzmR cells. Synergy was also observed against breast cancer stem cells. To determine if the combination is efficacious in inhibiting

Corresponding Author: Hui-Wen Lo, Ph.D., Department of Cancer Biology, Wake Forest University School of Medicine, 575 Patterson Ave, Suite 445, Winston-Salem, NC 27101, USA, hlo@wakehealth.edu; phone: 336-716-0695.
*These authors contributed equally.
#Current Address: Department of Biochemistry and Molecular Biology, Indiana University School of Medicine-Bloomington, JH 308 1001 E. 3rd St., Bloomington, IN 47405, USA

Competing Interest: None

Supplementary Materials and Methods, Supplementary Table I, and Supplementary Figs. 1 and 2 are available at *Oncogene*'s website.

metastasis, we treated mice with intracardially inoculated TNBC cells and found the combination to inhibit lung and liver metastases, and prolong host survival without toxicity. The combination inhibited orthotopic growth, VEGF-A expression, and tumor vasculature of both TNBC and HER2-positive trastuzumab-refractory breast cancer. Lung metastasis of orthotopic BT474-TtzmR xenografts was suppressed by the combination. Together, our results indicated that dual targeting of JAK2 and SMO resulted in synergistic suppression of breast cancer growth and metastasis, thereby supporting future clinical testing.

Keywords

JAK2; STAT3; SMO; GLI1; tGLI1; breast cancer; stem cells; metastasis

INTRODUCTION

Breast cancer is the most frequently diagnosed cancer in women with 1 in 8 at risks of developing invasive breast cancer over the course of her lifetime [1]. The National Cancer Institute reports that over 85% of patients diagnosed with localized or regional disease survive 5-years following their diagnosis; however, once distant metastases form, the 5-year survival rate plummets to 27% [2]. Breast cancers are classified based on the expression of immunohistochemical markers, such as, estrogen receptor (ER), progesterone receptor (PR), and the human epidermal growth factor receptor 2 (HER2). Of the five major molecular subtypes, the HER2-enriched (ER-/PR-/HER2+) and triple-negative (ER-/PR-/HER2-) subtypes are known to be more aggressive and have poorer outcomes due to increased probabilities of relapse and metastasis [3–6]. Five HER2-targeted agents have been approved by the United States Food and Drug Administration (FDA) for advanced HER2-positive breast cancer, namely, trastuzumab (Herceptin), lapatinib (Tykerb), pertuzumab (Perjet), ado-trastuzumab emtansine (Kadcyla), and most recently, fam-trastuzumab deruxtecan-nxki (Enhertu) [7–10]. However, most of the metastatic breast tumors that originally respond to HER2-targeted therapies typically develop resistance after one year. Due to the absence of ER, PR and HER2 expression in triple-negative breast cancers (TNBC), standard hormone therapies and HER2-targeted therapies are rendered ineffective. Instead, women with TNBC receive a combination of chemotherapy, radiation, and surgery [11, 12]. Unfortunately, chemotherapy has limited efficacy leading to residual disease following neoadjuvant therapy, relapse, metastasis, and a sharp decline in survival in the first 3–5 years after treatment [13]. Therefore, there is a clear need to identify novel therapeutics for TNBC and HER2-positive breast cancer.

Janus-activated kinase 2 (JAK2) is a non-receptor tyrosine kinase that is amplified and hyperactive in triple-negative and HER2-positive breast cancers [14, 15]. JAK2 serves as a signaling hub that integrates extracellular signals from interleukin receptors and oncogenic receptor tyrosine kinases to signal transducer and activator of transcription 3 (STAT3), an oncogenic transcription factor[16]. JAK2 phosphorylates STAT3 at Y705 permitting subsequent p-STAT3 homodimerization through interaction of their phosphorylated Y705 site and SH2 domain to induce its nuclear translocation and transcriptional activity [17, 18]. Nuclear STAT3 binds to its target gene promoters and upregulates expression of genes

involved in G1 cell cycle progression, proliferation, oncogenesis, anti-apoptosis, angiogenesis, and metastasis [19–23]. Additionally, we have reported the ability of STAT3 to upregulate expression of COX-2, iNOS, TWIST, and STAT1 [21–23]. Consistent with STAT3's role in promoting several oncogenic phenotypes, dysregulation of the JAK2-STAT3 pathway is associated with poor clinical outcomes and is being investigated as a therapeutic target [24, 25].

Smoothened (SMO) is an oncogenic 7-transmembrane receptor that activates the glioma-associated oncogene homolog 1 (GLI1) oncogenic transcription factors. SMO activity is constitutively repressed by the twelve-transmembrane receptor Patched1 and/or Patched2 (PTCH1 or PTCH2), however, this suppression is abolished upon binding of a Hedgehog family protein (Sonic, SHH; Indian, IHH; or Desert, DHH) to the PTCH receptors [26]. Once derepressed, SMO activates GLI transcription factors (GLI1, GLI2 and GLI3), which in turn activates expression of downstream target genes [27–29]. The SMO-GLI1 signaling axis plays an essential role in embryonic development, tissue regeneration, and stem cell renewal and its dysregulation has been implicated in tumorigenesis and vascular development [30, 31]. Our laboratory discovered an alternative splice variant of GLI1, termed truncated GLI1 (tGLI1) that presents with an in-frame deletion of 41 amino acids [32]. tGLI1 retains all known GLI1 functional domains, undergoes nuclear translocation, responds to SHH, and activates GLI1-target genes and functions as a gain-of-function transcription factor that promotes the aggressiveness of glioblastoma and breast cancer through increased migration, invasion, angiogenesis, and expression of stemness genes[33–38]. We have recently demonstrated that tGLI1 promotes breast cancer stem cells leading to breast cancer metastasis [38]. SMO has emerged as an important therapeutic target for several cancer types including breast cancer [39]. Two orally active SMO inhibitors, vismodegib (Erivedge) and sonidegib (Odzomo), received FDA approval for advanced basal cell carcinoma [40, 41]. Our laboratory previously reported that JAK2-STAT3 and SMO-GLI1/tGLI1 pathways are concurrently activated in most TNBC and HER2-enriched tumors [42], the two subtypes of breast cancer associated with most aggressive clinical behaviors. Furthermore, we demonstrated the novel finding that GLI1 and tGLI1 physically and functionally interact with STAT3 suggesting potential crosstalk to promote aggressiveness of TNBC and HER2-enriched breast cancer [42].

In this study, we tested novel combinations of FDA-approved JAK2-STAT3 and SMO-GLI1/tGLI1 pathway inhibitors for synergistic efficacy against triple-negative and HER2-positive breast cancer with acquired trastuzumab resistance to provide translatable results for developing novel therapies for these diseases. We observed that novel combinations synergized to suppress both basal and mesenchymal subtypes of TNBC and the luminal B (ER+/PR+/HER2+) BT474 cell line with acquired trastuzumab resistance. Several combinations effectively reduced the CD44^{high}/CD24^{low} MDA-231 cell population and the ability of basal TNBC BT20 to form mammospheres, suggesting these compounds suppressed the cancer stem cell population. Intracardiac and mammary fat pad xenograft animal models demonstrated that the pacritinib-sonidegib combination reduced the metastatic ability of circulating MDA-MB-231/MDA-231 and orthotopically growing MDA-231 and trastuzumab-resistant BT474 cells, respectively, through suppression of VEGF-A, mCD31, Ki-67, and p-STAT3. Collectively, our findings provide preclinical data

supporting the novel combination of JAK2-STAT3 and SMO-GLI1/tGLI1 inhibitors for treatment of TNBC and trastuzumab-resistant HER2-positive breast cancers.

MATERIALS AND METHODS

Cell lines and Reagents

Human breast cancer cell lines MCF10A, MDA-MB-468 (MDA-468), BT20, and MDA-MB-231 (MDA-231) were purchased from ATCC (Manassas, VA, USA) and cultured as instructed. Bone-metastatic MDA-MB-231BoM (231-BoM), and brain-metastatic MDA-MB-231BrM (231-BrM) cell lines are from the Massagué laboratory and were cultured in DMEM supplemented with 10% fetal bovine serum and 1% penicillin-streptomycin [43, 44]. Trastuzumab-resistant BT474 (BT474-TtzmR) were a kind gift from Dr. Dihua Yu [45]. All cell lines have been authenticated using the standard method, and tested for mycoplasma. If tested positive for mycoplasma contamination, cells were treated until free of contamination before use. Pacritinib, ruxolitinib, sonidegib, and vismodegib were obtained from AdooQ Bioscience (Irvine, CA, USA) and stock solutions were prepared using dimethyl sulfoxide (DMSO) for administration in cell culture.

Viability assay

Viability was determined using the CellTiter-Blue® Cell Viability Assay (Promega) according to the manufacturer's instructions. See supplementary material for details.

RESULTS

JAK2 and SMO inhibitors synergize to suppress TNBC and HER2-positive, trastuzumab-resistant breast cancers *in vitro*.

We previously demonstrated that the JAK2-STAT3 and SMO-GLI1/tGLI1 pathways are concurrently activated in TNBC and HER2-enriched breast cancer [42]. Given this observation, we reasoned that concurrent inhibition of these pathways may yield synergistic tumor cell kill. The FDA-approved JAK2 inhibitors, ruxolitinib (Rux) and pacritinib (Pac), and SMO inhibitors, vismodegib (Vis) and sonidegib (Son) were tested as single agents in MCF10A (immortalized mammary epithelial cells), MDA-468 (TNBC, basal), BT20 (TNBC, basal), MDA-231 (TNBC, mesenchymal), brain-metastatic MDA-231 (231-BrM; TNBC, mesenchymal), bone-metastatic MDA-231 (231-BoM; TNBC, mesenchymal), BT474 (Luminal B, HER2-positive), and trastuzumab-resistant BT474 (BT474-TtzmR; Luminal B, HER2-positive) cell lines to derive IC_{50} values (Fig. 1A). Cell lines were treated with a 5-point logarithmic dose curve spanning 0.01 μM to 100 μM for 48 hours before viability was measured using the CellTiter Blue assay. MCF10A cells had higher IC_{50}s for all four drugs except for BT474 cells treated with either JAK2 inhibitor and BT474-TtzmR cells treated with Rux. Additionally, JAK2 inhibitors tended to be more effective against triple negative cell lines compared to the luminal B cell lines, with the exception of Pac against the BT474-TtzmR cell line. We subsequently tested, for the first time, JAK2 and SMO inhibitors in combination at various ratios and determined the combination index (CI) using the Chou and Talalay method (CompuSyn)[46]. A combination index of less than one indicates synergy whereas a combination index greater than one indicates antagonism

between the inhibitors. The initial design of these experiments set the inhibitor dosage at the IC_{50} for each cell line and we further modified the ratio of the inhibitors to identify inhibitor ratios with efficacy. Multiple combinations yielded synergistic effects on all of the cell lines tested (Fig. 1B). For example, synergistic cell kill was observed in 3 of the 4 combinations tested in MDA-231 cells (Fig. 1C). Combinatorial treatment of ruxolitinib and either vismodegib or sonidegib significantly reduced MDA-231 viability compared to single agent treatments. MDA-231 viability was also significantly reduced when pacritinib and sonidegib were used in combination. This data suggests, for the first time, that simultaneous inhibition of the JAK2 and SMO pathways is more effective against TNBC and trastuzumab-resistant HER2-positive breast cancer than targeting either pathway alone.

Simultaneous inhibition of JAK2-STAT3 and SMO signaling pathways suppresses the cancer stem cell population.

STAT3 and GLI1/tGLI1 transcription factors promote renewal of cancer stem cells (CSCs), a subset of tumor cells thought to be the root cause of tumorigenesis, progression, drug resistance, and recurrence [37, 38, 47, 48]. Therefore, concurrent inhibition of the JAK2 and SMO signaling pathways should impact the CSC subpopulation. To investigate the effect of combinatorial JAK and SMO inhibitors, we performed flow cytometry to observe changes in the $CD44^{high}/CD24^{low}$ MDA-231 cell population following treatment (Fig. 2A–E). In breast cancer, patient-derived $CD44^{high}/CD24^{low}$ cells were found to be more tumorigenic than $CD44^{high}/CD24^{high}$ cells following implantation into the mammary fat pads of NOD-SCID mice[49]. The combinations of 1:5 pacritinib-sonidegib (Fig. 2B) and 10:1 ruxolitinib-sonidegib (Fig. 2C) significantly reduced the $CD44^{high}/CD24^{low}$ cell population compared to vehicle or any agent alone. Pacritinib-vismodegib combination treatment significantly reduced the $CD44^{high}/CD24^{low}$ cell population compared to the vehicle however, the combination was not more effective than pacritinib alone (Fig. 2D). Finally, the combination of 1:5 ruxolitinib-vismodegib had no effect on the $CD44^{high}/CD24^{low}$ cell population despite being synergistic in the viability assay (Fig. 2E). To further investigate dual inhibition of JAK2-STAT3 and SMO signaling pathways on CSCs, we treated BT20 mammospheres with JAK2 and SMO inhibitors alone and in combination. Pacritinib-sonidegib combination treatment significantly reduced the mammosphere-forming ability of BT20 cells compared to the vehicle or either agent alone (Fig. 2F). Interestingly, ruxolitinib-sonidegib combination treatment had no effect on mammosphere formation despite significantly suppressing the $CD44^{high}/CD24^{low}$ population (Fig. 2G). Pacritinib-vismodegib combination treatment was only more effective than vismodegib alone, which as a single agent, did not significantly suppress BT20 mammosphere formation compared to the vehicle (Fig. 2H). Finally, ruxolitinib-vismodegib combination significantly reduced mammosphere formation compared to vehicle or either agent alone (Fig. 2I). The pacritinib-sonidegib combination was selected for further study because these compounds had the lowest single agent IC_{50}s in MDA-231 cells, suppressed the $CD44^{high}/CD24^{low}$ MDA-231 cell population, and inhibited mammosphere formation of BT20 and MDA-468 cells (Supplementary Fig. 1). Consistent with the BT20 mammosphere assay, formation of BT474-TtzmR mammospheres was significantly reduced with pacritinib-sonidegib combination therapy (Fig. 2J). Despite previously reporting the functional interaction between STAT3 and GLI1/tGLI1, the combination treatment did not reduce the STAT3-

GLI1/tGLI1 interaction as determined by immunoprecipitation western blot (Supplementary Fig. 2). Together, these results indicated that simultaneous inhibition of JAK2-STAT3 and SMO signaling pathways suppress CSCs.

Co-treatment with JAK2 and SMO inhibitors suppresses the orthotopic growth of TNBC tumors *in vivo*.

To assess pacritinib-sonidegib synergism *in vivo*, luciferase-expressing MDA-231 breast cancer cells were implanted into the mammary fat pads (MFP) of female nude mice. Tumors were allowed to reach about 100 mm^3, and then randomized to receive vehicle, pacritinib (7.5 mg/kg; ip), sonidegib (20 mg/kg; ip), or pacritinib-sondiegib combination. Mice were then treated for 20 days (N=9–10 mice/group). Primary tumor size was determined by caliper measurements and metastasis formation was monitored by bioluminescent imaging (Fig. 3A). Tumor growth was significantly reduced with combination therapy compared to vehicle whereas single agents did not significantly alter tumor growth (Figs. 3B–C). *In vivo* bioluminescent imaging revealed the formation of distant metastases, so organs of inoculated mice were harvested to determine the effect of JAK2 and SMO inhibition on distant metastasis. However, there was no discernable difference in the occurrence of distant metastases across treatment groups (Fig. 3D–H). The single agent and combination treatments were well tolerated because we observed no significant variations in body weight compared to vehicle throughout the study (Fig. 3I). Collectively, these findings suggest that combined inhibition of JAK2 and SMO signaling pathways synergize to slow the growth of TNBC tumors *in vivo*.

Combined treatment with JAK2 and SMO inhibitors reduces TNBC metastasis *in vivo*.

Since breast CSCs are considered the metastasis-initiating cells, we next investigated whether our *in vitro* findings that simultaneous inhibition of JAK2-STAT3 and SMO-GLI1/tGLI1 signaling pathways inhibited the CSC subpopulation could be recapitulated *in vivo* [50]. We determined the efficacy of pacritinib-sonidegib combination treatment against TNBC metastasis using an intracardiac mouse model which mimics several stages of metastasis including evasion of anoikis, intravasation, and colonization to distant organs, mainly to the brain and bone. Luciferase-expressing MDA-231 cells were injected into the left ventricle of anesthetized athymic nude mice which were randomized into treatment groups of vehicle, pacritinib (7.5 mg/kg; ip), sonidegib (20 mg/kg; ip), or pacritinib-sonidegib combination treatment beginning 3 days post-inoculation (Fig. 4A). Mice treated with the combination therapy presented with reduced overall tumor burden compared to the vehicle treatment or either single agent alone (Fig. 4B). Additionally, the mice treated with the combination therapy had a significantly better overall survival compared to single treatment or vehicle groups (Fig. 4C). The single and combination treatments were well tolerated because body weight showed no significant differences compared to vehicle throughout the study (Fig. 4D). Representative *ex vivo* bioluminescent organ images demonstrated that pacritinib-sonidegib combination treatment also effectively reduced the frequency of detectable organ-specific metastases in inoculated mice (Fig. 4E–F). Combination therapy drastically reduced the incidence of lung metastasis compared to the vehicle and either single agent, from 67–78% to 13%, respectively (N=8–9 mice/group). The incidence of liver and bone metastasis also decreased with combination therapy compared to

the vehicle and pacritinib only groups while the incidence of these metastases in the group treated with sonidegib alone was similar to the combination treatment. Conversely, the frequency of brain metastases was relatively consistent across all treatment groups. Quantification of *ex vivo* organ bioluminescence revealed the combination therapy significantly reduced the size of lung (Fig. 4G) and liver (Fig. 4H) metastases while the size of brain (Fig. 4I) and bone (Fig. 4J) metastases were not affected by the combination therapy. These findings demonstrated, for the first time, that simultaneous inhibition of JAK2-STAT3 and SMO-GLI1/tGLI1 signaling reduces TNBC metastasis.

Co-treatment with JAK2 and SMO inhibitors suppresses the growth and lung metastasis of HER2-positive trastuzumab-resistant breast cancer *in vivo*.

In vitro experiments testing novel combinations of JAK2 and SMO inhibitors revealed synergistic cell kill in a HER2-positive breast cancer cell line with acquired trastuzumab resistance (BT474-TtzmR). We observed synergism between ruxolitinib in combination with either vismodegib or sonidegib, and between pacritinib and sonidegib in BT474-TtzmR cells (Fig. 1B). Even though ruxolitinib synergized with both SMO inhibitors in this cell line, pacritinib-sonidegib combination in this *in vivo* model because the IC_{50} of pacritinib was substantially lower than ruxolitinib, 0.8 μM versus 57 μM, respectively, in the BT474-TtzmR cell line (Fig. 1A). Therefore, to test our findings *in vivo*, luciferase-expressing BT474-TtzmR breast cancer cells were implanted into MFP of nude mice. Tumors were allowed to establish for 18 days after which the average tumor size was 90.2 ± 14.9 mm^3. Mice were then randomized to receive vehicle, pacritinib (7.5 mg/kg; ip), sonidegib (20 mg/kg; ip), or pacritinib-sonidegib combination and mice were then treated for 32 days (N=8–9 mice/group). Primary tumor size was determined by caliper measurements and secondary metastasis formation was monitored by bioluminescent imaging (Fig. 5A). Tumor growth was significantly reduced with combination therapy compared to vehicle whereas single agents did not significantly alter tumor growth (Figs. 5B–C). Tumors treated with combination therapy tended to be smaller than those treated with either pacritinib or sonidegib alone; however, these comparisons did not reach significance. *In vivo* bioluminescent imaging over the course of the study revealed the formation of distant metastases, so the organs of inoculated mice were harvested to determine the effect of JAK2 and SMO inhibition on metastatic organotropism of trastuzumab-resistant BT474 breast cancer cells. Lung metastases were not detected in mice treated with pacritinib-sonidegib combination therapy while they were readily found in those treated with either inhibitor alone (Fig. 5D–E). Additionally, combination therapy did not inhibit formation of either bone or liver metastases when compared to the other treatment groups. Quantification of the *ex vivo* organ bioluminescent signal revealed that the combination therapy significantly reduced the size of lung metastases (Fig. 5F), but not bone (Fig. 5G) or liver metastases (Fig. 5H). The single and combination treatments were well tolerated by the mice in this study as body weight showed no significant differences compared to vehicle throughout the study (Fig. 5I). Furthermore, neither single agent treatment nor the combination therapy caused a significant increase in alanine transaminase (ALT) activity compared to the vehicle control (Fig. 5J). Circulating ALT activity for all treatments groups was below the activity level found in nude mice treated with sublethal doses of thioacetamide, a compound known to induce hepatocellular injury[51]. Together, these results indicated that the novel combination

of JAK2 and SMO inhibitors suppressed the growth and lung metastasis of HER2-positive trastuzumab-resistant breast cancer *in vivo*.

Combined treatment with JAK2 and SMO inhibitors synergize to reduce angiogenesis, tumor cell proliferation, and tumoral STAT3 activation of TNBC *in vivo*.

To determine the mechanism by which the pacritinib-sonidegib combination therapy inhibited the growth of MDA-231 and BT474-TtzmR MFP tumors, we examined target genes that have been previously shown to be modulated by both JAK2-STAT3 and SMO-GLI1/tGLI1 signaling. Bcl-2 [52, 53], Nanog [38, 54, 55], and VEGF-A [56, 57] were selected as potential biomarkers of pacritinib-sonidegib synergism. Gene expression analysis of MDA-231 cells treated with pacritinib alone sonidegib alone, or the two in combination revealed synergistic downregulation of Bcl-2. (Fig. 6A). We then sought to validate this biomarker through immunohistochemistry (IHC) analysis of treated MFP tumors. In contrast to the decrease in Bcl-2 gene expression with combination treatment, we observed a significant increase in Bcl-2 protein expression with combination treatment compared to vehicle and either single agent (Figs. 6B–C). In light of this conflicting evidence, we then stained the tumors for VEGF-A expression and observed that the combination significantly reduced VEGF-A expression compared to the untreated controls and both single agents (Figs. 6B, D). Given the marked decrease in VEGF-A expression, an important mediator of neovascularization, we further characterized the tumor vasculature by assessing mCD31 expression for endothelial cells. IHC analysis of tumor sections revealed a significant decrease in microvessel density with the combination treatment (Figs. 6B, E). Further characterization of the proliferative index (% Ki-67 positive cells) of the MFP tumors showed that the number of actively proliferating cells was significantly reduced by the combination treatment (Figs. 6B, F). Furthermore, the combination of pacritinib and sonidegib synergized to significantly reduce the expression of activated STAT3 (p-STAT3 Y705) compared to the vehicle and both single agents (Figs. 6B, G). Interestingly, there was no significant increase in apoptosis as determined by TUNEL assay (Fig. 6H). Collectively, these data suggest the pacritinib-sonidegib combination treatment reduces MDA-231 tumor growth primarily by reducing VEGF-A expression, angiogenesis, and tumor cell proliferation.

JAK2 and SMO inhibitors synergize to reduce tumor cell proliferation and tumoral STAT3 activation, and induce apoptosis of HER2-positive trastuzumab-resistant breast cancer *in vivo*.

To determine the mechanism by which the pacritinib-sonidegib combination therapy inhibited trastuzumab-resistant breast cancer *in vivo* (Fig. 5), we characterized the treated MFP tumors for target gene protein expression, proliferation, p-STAT3 expression, and apoptosis. RT-qPCR analysis of BT474-TtzmR cells *in vitro* identified Nanog and VEGF-A as potential biomarkers (Fig. 7A). *In vivo*, VEGF-A protein expression was significantly decreased by the combination treatment compared to the untreated controls and both single agent treatments (Fig. 7B–C). Further characterization of endothelial cells within the tumor microenvironment by mCD31 IHC staining revealed that pacritinib and sonidegib synergized to further decrease the microvessel density of treated tumors (Figs. 7B, D). All three treatments significantly reduced the proliferative index compared to the control group

(Figs. 7B, E). Furthermore, combination treatment significantly reduced the number of p-STAT3 (Y705)-positive cells compared to the vehicle treatment while single agent treatments did not significantly reduce the p-STAT3 status (Figs. 7B, F). There was no significant increase in apoptosis as determined by TUNEL assay (Figs. 7G–H). These results, together, indicate that the combination treatment inhibited BT474-TtzmR tumor growth primarily through reducing VEGF-A expression, tumor angiogenesis, and cell proliferation.

DISCUSSION

In this study, we report for the first time that novel combinations of JAK2 and SMO inhibitors synergize to suppress the growth and metastasis of TNBC and HER2-positive trastuzumab-resistant breast cancer cell lines. Several of these combinations suppressed the CD44^{high}/CD24^{low} cell population and inhibited mammosphere formation of TNBC cells. Using a TNBC mouse model of experimental metastasis, we demonstrated that pacritinib-sonidegib combination therapy slowed MDA-231 xenograft growth, and increased overall survival and inhibited lung and liver metastasis of MDA-231 cells. Furthermore, the pacritinib-sondiegib combination therapy significantly reduced the orthotopic growth of trastuzumab-resistant HER2-positive BT474-TtzmR xenografts. Xenograft characterization further revealed a decrease in angiogenesis, Ki-67 positivity, and p-STAT3 expression following pacritinib-sondiegib combination treatment.

Both JAK2 and SMO have emerged as important therapeutic targets for several cancers including breast cancer; however, these agents have been employed primarily as either single agents or in combination with chemotherapeutics [14, 15, 39]. Ruxolitinib is approved by the FDA for treatment of myelofibrosis and polycythemia vera. Ruxolitinib is being investigated for use in TNBC as a single agent and in combination with capecitabine; however, neither therapeutic strategy resulted in significant patient benefit in phase II trials (NCT01562873, NCT02120417). Additional trials are investigating the use of ruxolitinib in combination with pembrolizumab in stage IV TNBC (NCT03012230). For metastatic HER2-positive breast cancer, ruxolitinib in combination with herceptin is in a phase I/II clinical trial (NCT02066532). The dose-limiting myelosuppression that frequently accompanies ruxolitinib treatment inspired the search for JAK inhibitors with a reduced risk of adverse events. Pacritinib, another JAK2 inhibitor with similar potency against JAK2 and FLT3 which lacks myelosuppressive activity, is currently undergoing trials for leukemias, myelofibrosis, and graft versus host disease. Previous trials investigating pacritinib in colon and lung cancers were terminated due to a clinical hold placed on pacritinib by the FDA as a result of increased side effects and drug shortages, respectively (NCT02277093, NCT02342353). Pacritinib is now being investigated in a phase II clinical trial in patients with myelofibrosis who were previously treated with ruxolitinib (NCT03165734). Despite preclinical evidence that JAK inhibition disrupts progression of breast cancer in xenograft models, there are currently no clinical trials for pacritinib in breast cancer patients[58]. In light of continued observation of serious adverse events in patients treated with JAK inhibitors, the clinical success of these compounds in treating solid tumors may rely on their synergism with orthogonal therapeutics to reduce the patient's total drug exposure.

Two orally active SMO inhibitors, sonidegib and vismodegib, received FDA approval for advanced basal cell carcinoma. In these patients, cell autonomous activation of the Hedgehog pathway arises from loss-of-function of *PTCH1* (90%) or gain-of-function of SMO (10%) resulting in SMO hyperactivity [59]. Despite this actionable SMO dysregulation, these tumors frequently develop resistance to SMO inhibitors via novel SMO mutations or by upregulating additional pathways that activate GLI1 downstream of SMO including PI3K/AKT, RAS/RAF/MEK/ERK, and TGF-β [60, 61]. *PTCH1* mutations are rare in breast cancer arguing against mutational activation of the Hedgehog pathway and precluding the efficacy of SMO antagonists when employed as single agents [62, 63]. Sonidegib in combination with docetaxel was tested in a phase I clinical trial for advanced breast cancer in which patients receiving up to 800 mg daily experienced no dose limiting toxicities [64]. Unfortunately, a trial investigating sonidegib in TNBC was withdrawn due to poor accrual (NCT01757327). On the other hand, vismodegib is being evaluated with the chemotherapeutic agents paclitaxel, epirubicin, and cyclophosphamide, in a phase II trial (NCT02694224).

Our previous findings demonstrating the novel physical and functional interactions of STAT3 and GLI1/tGLI1 provided the rationale for simultaneous inhibition of the JAK2-STAT3 and SMO-GLI1/tGLI1 signaling axes to achieve optimal clinical efficacy for triple-negative and trastuzumab-refractory HER2-positive breast cancers. Despite both JAK2 and SMO inhibitors being known to induce apoptosis, we did not detect a significant increase in apoptosis following co-treatment with sonidegib and pacritinib in our orthotopic xenograft mouse model utilizing the trastuzumab-resistant HER2-positive breast cancer cell line BT474-TtzmR [47, 65, 66]. We speculate this may be due to the involvement of HER2 signaling which has been shown to inhibit apoptosis in breast cancer [67, 68].

Given that both pathways are known to promote CSCs, the reduction in tumor growth observed in our mouse model may be attributed to inhibition of the CSC population. STAT3 has been shown to be dysregulated in CSCs and directly upregulate several transcription factors intimately involved in maintaining cell pluripotency including c-Myc, SOX2, and Nanog [69–72]. Marotta et al. demonstrated the IL-6/JAK2/STAT3 signaling axis was preferentially active in CD44^{high}/CD24^{low} breast cancer cells with subsequent JAK2 inhibition reducing the CD44^{high}/CD24^{low} population and xenograft tumor growth [73]. In our hands, inhibition of IL-6/JAK2/STAT3 signaling also reduced the CD44^{high}/CD24^{low} breast cancer cell population (Fig. 2). Our laboratory has previously demonstrated the SMO-GLI1/tGLI1 signaling axis to mediate the CSC population of both glioblastoma and breast cancer [37, 38]. Overexpression of tGLI1 significantly increased the CD44^{high}/CD24^{low} breast cancer cell population, mammosphere formation, and expression of the stemness genes Nanog, SOX2, and OCT4 in both HER2-enriched and TNBC cell lines[38]. It remains plausible that CSCs may overcome inhibition of either JAK2-STAT3 or SMO-GLI1/tGLI1 signaling through upregulation of the other to maintain their stem-like phenotype and self-renewal capabilities. Therefore, as demonstrated above, simultaneous inhibition of both signaling pathways yields synergistic inhibition of CSCs, tumor growth, and metastasis.

Both the JAK2-STAT3 and SMO-GLI1/tGLI1 signaling axes are known to crosstalk with the Hippo pathway [74–76]. The Hippo signaling pathway is routinely described as a tumor

suppressor pathway due to its control over cellular proliferation, survival, and differentiation [77, 78]. Inactivation of the Hippo pathway permits the nuclear translocation of TAZ/YAP allowing these kinases to function as transcriptional co-activators through association with DNA-binding proteins to drive gene transcription. In pancreatic cancer, Gruber *et al.* showed the *KRas^{G12D}* mutation activated YAP1 and TAZ signaling which increased transcription of STAT3 [79]. Previous studies have shown that YAP1 overexpression leads to malignant transformation of human mammary epithelial cells [80]. Sonic hedgehog-driven medulloblastomas in both humans and mice present with high expression of YAP1 and its transcriptional partner TEAD [76]. Furthermore, sonic hedgehog signaling regulates YAP1 nuclear localization by promoting its interaction with IRS1 [76]. Given this crosstalk, future studies elucidating the efficacy of Hippo pathway inhibitors in combination with JAK2-STAT3 and/or SMO-GLI1/tGLI1 inhibitors are needed.

In conclusion, we provide novel evidence that simultaneous inhibition of the JAK2-STAT3 and SMO-GLI1/tGLI1 signaling axes synergize to suppress TNBC and trastuzumab-refractory HER2-positive breast cancers. Combination treatment of the JAK2 inhibitor pacritinib and the SMO inhibitor sonidegib significantly reduced the metastatic potential of triple-negative breast cancer *in vivo*. This combination also significantly reduced trastuzumab-resistant HER2-positive primary tumor growth and the formation of secondary metastases with limited toxicity. This preclinical data provides the basis for future clinical development of novel targeted combination therapies for TNBC and trastuzumab-resistant HER2-positive breast cancers.

Supplementary Material

Refer to Web version on PubMed Central for supplementary material.

ACKNOWLEDGEMENTS

REFERENCES

1. Siegel RL, Miller KD, Jemal A. Cancer statistics, 2020. CA: A Cancer Journal for Clinicians 2020; 70: 7–30. [PubMed: 31912902]

2. Howlader NNA, Krapcho M, Miller D, Brest A, Yu M, Ruhl J, Tatalovich Z, Mariotto A, Lewis DR, Chen HS, Feuer EJ, Cronin KA (eds). SEER Cancer Statistics Review, 1975–2016, National Cancer Institute. Bethesda, MD, https://seer.cancer.gov/csr/1975_2016/, based on November 2018 SEER data submission, posted to the SEER web site, April 2019., vol. 2020, 1975–2016.

3. Perou CM, Sorlie T, Eisen MB, van de Rijn M, Jeffrey SS, Rees CA et al. Molecular portraits of human breast tumours. Nature 2000; 406: 747–752. [PubMed: 10963602]

4. Fan C, Oh DS, Wessels L, Weigelt B, Nuyten DS, Nobel AB et al. Concordance among gene-expression-based predictors for breast cancer. The New England journal of medicine 2006; 355: 560–569. [PubMed: 16899776]

5. Kuba S, Ishida M, Nakamura Y, Yamanouchi K, Minami S, Taguchi K et al. Treatment and prognosis of breast cancer patients with brain metastases according to intrinsic subtype. Jpn J Clin Oncol 2014; 44: 1025–1031. [PubMed: 25156682]

6. Paik S, Hazan R, Fisher ER, Sass RE, Fisher B, Redmond C et al. Pathologic findings from the National Surgical Adjuvant Breast and Bowel Project: prognostic significance of erbB-2 protein overexpression in primary breast cancer. Journal of clinical oncology : official journal of the American Society of Clinical Oncology 1990; 8: 103–112. [PubMed: 1967301]

7. Cobleigh MA, Vogel CL, Tripathy D, Robert NJ, Scholl S, Fehrenbacher L et al. Multinational study of the efficacy and safety of humanized anti-HER2 monoclonal antibody in women who have HER2-overexpressing metastatic breast cancer that has progressed after chemotherapy for metastatic disease. Journal of clinical oncology : official journal of the American Society of Clinical Oncology 1999; 17: 2639–2648. [PubMed: 10561337]

8. Ryan Q, Ibrahim A, Cohen MH, Johnson J, Ko C-w, Sridhara R et al. FDA Drug Approval Summary: Lapatinib in Combination with Capecitabine for Previously Treated Metastatic Breast Cancer That Overexpresses HER-2. The oncologist 2008; 13: 1114–1119. [PubMed: 18849320]

9. Howie LJ, Scher NS, Amiri-Kordestani L, Zhang L, King-Kallimanis BL, Choudhry Y et al. FDA Approval Summary: Pertuzumab for Adjuvant Treatment of HER2-Positive Early Breast Cancer. Clin Cancer Res 2019; 25: 2949–2955. [PubMed: 30552112]

10. Baron JM, Boster BL, Barnett CM. Ado-trastuzumab emtansine (T-DM1): a novel antibody-drug conjugate for the treatment of HER2-positive metastatic breast cancer. Journal of oncology pharmacy practice : official publication of the International Society of Oncology Pharmacy Practitioners 2015; 21: 132–142. [PubMed: 24682654]

11. Al-Mahmood S, Sapiezynski J, Garbuzenko OB, Minko T. Metastatic and triple-negative breast cancer: challenges and treatment options. Drug Deliv Transl Res 2018; 8: 1483–1507. [PubMed: 29978332]

12. Lebert JM, Lester R, Powell E, Seal M, McCarthy J. Advances in the systemic treatment of triple-negative breast cancer. Current oncology (Toronto, Ont) 2018; 25: S142–s150.

13. Palmieri C, Krell J, James CR, Harper-Wynne C, Misra V, Cleator S et al. Rechallenging with anthracyclines and taxanes in metastatic breast cancer. Nature reviews Clinical oncology 2010; 7: 561–574.

14. Balko JM, Giltnane JM, Wang K, Schwarz LJ, Young CD, Cook RS et al. Molecular profiling of the residual disease of triple-negative breast cancers after neoadjuvant chemotherapy identifies actionable therapeutic targets. Cancer Discov 2014; 4: 232–245. [PubMed: 24356096]

15. Balko JM, Schwarz LJ, Luo N, Estrada MV, Giltnane JM, Davila-Gonzalez D et al. Triple-negative breast cancers with amplification of JAK2 at the 9p24 locus demonstrate JAK2-specific dependence. Sci Transl Med 2016; 8: 334ra353.

16. Loh CY, Arya A, Naema AF, Wong WF, Sethi G, Looi CY. Signal Transducer and Activator of Transcription (STATs) Proteins in Cancer and Inflammation: Functions and Therapeutic Implication. Frontiers in oncology 2019; 9: 48. [PubMed: 30847297]

17. Johnson DE, O'Keefe RA, Grandis JR. Targeting the IL-6/JAK/STAT3 signalling axis in cancer. Nature reviews Clinical oncology 2018; 15: 234–248.

18. Wang Y, Shen Y, Wang S, Shen Q, Zhou X. The role of STAT3 in leading the crosstalk between human cancers and the immune system. Cancer letters 2018; 415: 117–128. [PubMed: 29222039]

19. Guo C, Chang CC, Wortham M, Chen LH, Kernagis DN, Qin X et al. Global identification of MLL2-targeted loci reveals MLL2's role in diverse signaling pathways. Proceedings of the National Academy of Sciences of the United States of America 2012; 109: 17603–17608. [PubMed: 23045699]

20. Lo HW, Cao X, Zhu H, Ali-Osman F. Constitutively activated STAT3 frequently coexpresses with epidermal growth factor receptor in high-grade gliomas and targeting STAT3 sensitizes them to Iressa and alkylators. Clin Cancer Res 2008; 14: 6042–6054. [PubMed: 18829483]

21. Lo H-W, Cao X, Zhu H, Ali-Osman F. Cyclooxygenase-2 is a novel transcriptional target of the nuclear EGFR-STAT3 and EGFRvIII-STAT3 signaling axes. Molecular cancer research : MCR 2010; 8: 232–245. [PubMed: 20145033]

22. Lo HW, Hsu SC, Xia W, Cao X, Shih JY, Wei Y et al. Epidermal growth factor receptor cooperates with signal transducer and activator of transcription 3 to induce epithelial-mesenchymal transition in cancer cells via up-regulation of TWIST gene expression. Cancer research 2007; 67: 9066–9076. [PubMed: 17909010]

23. Lo HW, Hsu SC, Ali-Seyed M, Gunduz M, Xia W, Wei Y et al. Nuclear interaction of EGFR and STAT3 in the activation of the iNOS/NO pathway. Cancer cell 2005; 7: 575–589. [PubMed: 15950906]

24. Kusaba T, Nakayama T, Yamazumi K, Yakata Y, Yoshizaki A, Inoue K et al. Activation of STAT3 is a marker of poor prognosis in human colorectal cancer. Oncol Rep 2006; 15: 1445–1451. [PubMed: 16685378]

25. Qin J-J, Yan L, Zhang J, Zhang W-D. STAT3 as a potential therapeutic target in triple negative breast cancer: a systematic review. Journal of Experimental & Clinical Cancer Research 2019; 38: 195. [PubMed: 31088482]

26. Riobo-Del Galdo NA, Lara Montero Á, Wertheimer EV. Role of Hedgehog Signaling in Breast Cancer: Pathogenesis and Therapeutics. Cells 2019; 8: 375.

27. Clement V, Sanchez P, de Tribolet N, Radovanovic I, Ruiz i Altaba A. HEDGEHOG-GLI1 signaling regulates human glioma growth, cancer stem cell self-renewal, and tumorigenicity. Current biology : CB 2007; 17: 165–172. [PubMed: 17196391]

28. Fiaschi M, Rozell B, Bergstrom A, Toftgard R. Development of mammary tumors by conditional expression of GLI1. Cancer research 2009; 69: 4810–4817. [PubMed: 19458072]

29. Kinzler KW, Ruppert JM, Bigner SH, Vogelstein B. The GLI gene is a member of the Kruppel family of zinc finger proteins. Nature 1988; 332: 371–374. [PubMed: 2832761]

30. Machold R, Hayashi S, Rutlin M, Muzumdar MD, Nery S, Corbin JG et al. Sonic hedgehog is required for progenitor cell maintenance in telencephalic stem cell niches. Neuron 2003; 39: 937–950. [PubMed: 12971894]

31. Liu S, Dontu G, Mantle ID, Patel S, Ahn NS, Jackson KW et al. Hedgehog signaling and Bmi-1 regulate self-renewal of normal and malignant human mammary stem cells. Cancer research 2006; 66: 6063–6071. [PubMed: 16778178]

32. Lo HW, Zhu H, Cao X, Aldrich A, Ali-Osman F. A novel splice variant of GLI1 that promotes glioblastoma cell migration and invasion. Cancer research 2009; 69: 6790–6798. [PubMed: 19706761]

33. Cao X, Geradts J, Dewhirst MW, Lo HW. Upregulation of VEGF-A and CD24 gene expression by the tGLI1 transcription factor contributes to the aggressive behavior of breast cancer cells. Oncogene 2012; 31: 104–115. [PubMed: 21666711]

34. Han W, Carpenter RL, Lo H-W. TGLI1 Upregulates Expression of VEGFR2 and VEGF-A, Leading to a Robust VEGF-VEGFR2 Autocrine Loop and Cancer Cell Growth. Cancer Hallmarks 2013; 1: 28–37.

35. Zhu H, Carpenter RL, Han W, Lo HW. The GLI1 splice variant TGLI1 promotes glioblastoma angiogenesis and growth. Cancer letters 2014; 343: 51–61. [PubMed: 24045042]

36. Carpenter RL, Paw I, Zhu H, Sirkisoon S, Xing F, Watabe K et al. The gain-of-function GLI1 transcription factor TGLI1 enhances expression of VEGF-C and TEM7 to promote glioblastoma angiogenesis. Oncotarget 2015; 6: 22653–22665. [PubMed: 26093087]

37. Rimkus TK, Carpenter RL, Sirkisoon S, Zhu D, Pasche BC, Chan MD et al. Truncated Glioma-Associated Oncogene Homolog 1 (tGLI1) Mediates Mesenchymal Glioblastoma via Transcriptional Activation of CD44. Cancer research 2018; 78: 2589–2600. [PubMed: 29463580]

38. Sirkisoon SR, Carpenter RL, Rimkus T, Doheny D, Zhu D, Aguayo NR et al. TGLI1 transcription factor mediates breast cancer brain metastasis via activating metastasis-initiating cancer stem cells and astrocytes in the tumor microenvironment. Oncogene 2020; 39: 64–78. [PubMed: 31462709]

39. Kameda C, Tanaka H, Yamasaki A, Nakamura M, Koga K, Sato N et al. The Hedgehog pathway is a possible therapeutic target for patients with estrogen receptor-negative breast cancer. Anticancer research 2009; 29: 871–879. [PubMed: 19414322]

40. Aditya S, Rattan A. Vismodegib: A smoothened inhibitor for the treatment of advanced basal cell carcinoma. Indian Dermatol Online J 2013; 4: 365–368. [PubMed: 24350028]

41. Jain S, Song R, Xie J. Sonidegib: mechanism of action, pharmacology, and clinical utility for advanced basal cell carcinomas. OncoTargets and therapy 2017; 10: 1645–1653. [PubMed: 28352196]

42. Sirkisoon SR, Carpenter RL, Rimkus T, Anderson A, Harrison A, Lange AM et al. Interaction between STAT3 and GLI1/tGLI1 oncogenic transcription factors promotes the aggressiveness of triple-negative breast cancers and HER2-enriched breast cancer. Oncogene 2018; 37: 2502–2514. [PubMed: 29449694]

43. Bos PD, Zhang XH, Nadal C, Shu W, Gomis RR, Nguyen DX et al. Genes that mediate breast cancer metastasis to the brain. Nature 2009; 459: 1005–1009. [PubMed: 19421193]

44. Kang Y, Siegel PM, Shu W, Drobnjak M, Kakonen SM, Cordón-Cardo C et al. A multigenic program mediating breast cancer metastasis to bone. Cancer cell 2003; 3: 537–549. [PubMed: 12842083]

45. Zhang S, Huang WC, Li P, Guo H, Poh SB, Brady SW et al. Combating trastuzumab resistance by targeting SRC, a common node downstream of multiple resistance pathways. Nat Med 2011; 17: 461–469. [PubMed: 21399647]

46. Chou TC, Talalay P. Quantitative analysis of dose-effect relationships: the combined effects of multiple drugs or enzyme inhibitors. Advances in enzyme regulation 1984; 22: 27–55. [PubMed: 6382953]

47. Carpenter RL, Lo HW. STAT3 Target Genes Relevant to Human Cancers. Cancers 2014; 6: 897–925. [PubMed: 24743777]

48. Merchant AA, Matsui W. Targeting Hedgehog--a cancer stem cell pathway. Clin Cancer Res 2010; 16: 3130–3140. [PubMed: 20530699]

49. Al-Hajj M, Wicha MS, Benito-Hernandez A, Morrison SJ, Clarke MF. Prospective identification of tumorigenic breast cancer cells. Proceedings of the National Academy of Sciences 2003; 100: 3983–3988.

50. Wang T, Shigdar S, Gantier MP, Hou Y, Wang L, Li Y et al. Cancer stem cell targeted therapy: progress amid controversies. Oncotarget 2015; 6: 44191–44206. [PubMed: 26496035]

51. Ackerman Z, Pappo O, Link G, Glazer M, Grozovski M. Liver toxicity of thioacetamide is increased by hepatocellular iron overload. Biological trace element research 2015; 163: 169–176. [PubMed: 25161090]

52. Choi HJ, Han JS. Overexpression of phospholipase D enhances Bcl-2 expression by activating STAT3 through independent activation of ERK and p38MAPK in HeLa cells. Biochim Biophys Acta 2012; 1823: 1082–1091. [PubMed: 22504301]

53. Bigelow RL, Chari NS, Unden AB, Spurgers KB, Lee S, Roop DR et al. Transcriptional regulation of bcl-2 mediated by the sonic hedgehog signaling pathway through gli-1. The Journal of biological chemistry 2004; 279: 1197–1205. [PubMed: 14555646]

54. Bourguignon LY, Peyrollier K, Xia W, Gilad E. Hyaluronan-CD44 interaction activates stem cell marker Nanog, Stat-3-mediated MDR1 gene expression, and ankyrin-regulated multidrug efflux in breast and ovarian tumor cells. The Journal of biological chemistry 2008; 283: 17635–17651. [PubMed: 18441325]

55. Zbinden M, Duquet A, Lorente-Trigos A, Ngwabyt SN, Borges I, Ruiz i Altaba A. NANOG regulates glioma stem cells and is essential in vivo acting in a cross-functional network with GLI1 and p53. EMBO J 2010; 29: 2659–2674. [PubMed: 20581802]

56. Niu G, Wright KL, Huang M, Song L, Haura E, Turkson J et al. Constitutive Stat3 activity up-regulates VEGF expression and tumor angiogenesis. Oncogene 2002; 21: 2000–2008. [PubMed: 11960372]

57. Chen W, Tang T, Eastham-Anderson J, Dunlap D, Alicke B, Nannini M et al. Canonical hedgehog signaling augments tumor angiogenesis by induction of VEGF-A in stromal perivascular cells. Proceedings of the National Academy of Sciences 2011; 108: 9589–9594.

58. Tavallai M, Booth L, Roberts JL, Poklepovic A, Dent P. Rationally Repurposing Ruxolitinib (Jakafi ((R))) as a Solid Tumor Therapeutic. Frontiers in oncology 2016; 6: 142. [PubMed: 27379204]

59. Epstein EH. Basal cell carcinomas: attack of the hedgehog. Nature Reviews Cancer 2008; 8: 743–754. [PubMed: 18813320]

60. Atwood SX, Sarin KY, Whitson RJ, Li JR, Kim G, Rezaee M et al. Smoothened variants explain the majority of drug resistance in basal cell carcinoma. Cancer cell 2015; 27: 342–353. [PubMed: 25759020]

61. Teperino R, Aberger F, Esterbauer H, Riobo N, Pospisilik JA. Canonical and non-canonical Hedgehog signalling and the control of metabolism. Semin Cell Dev Biol 2014; 33: 81–92. [PubMed: 24862854]

62. Xie J, Johnson RL, Zhang X, Bare JW, Waldman FM, Cogen PH et al. Mutations of the PATCHED gene in several types of sporadic extracutaneous tumors. Cancer research 1997; 57: 2369–2372. [PubMed: 9192811]

63. Jiao X, Wood LD, Lindman M, Jones S, Buckhaults P, Polyak K et al. Somatic mutations in the Notch, NF-KB, PIK3CA, and Hedgehog pathways in human breast cancers. Genes Chromosomes Cancer 2012; 51: 480–489. [PubMed: 22302350]

64. Ruiz-Borrego M, Jimenez B, Antolin S, Garcia-Saenz JA, Corral J, Jerez Y et al. A phase Ib study of sonidegib (LDE225), an oral small molecule inhibitor of smoothened or Hedgehog pathway, in combination with docetaxel in triple negative advanced breast cancer patients: GEICAM/2012–12 (EDALINE) study. Investigational new drugs 2019; 37: 98–108. [PubMed: 29948356]

65. Zaidi AH, Komatsu Y, Kelly LA, Malhotra U, Rotoloni C, Kosovec JE et al. Smoothened inhibition leads to decreased proliferation and induces apoptosis in esophageal adenocarcinoma cells. Cancer Invest 2013; 31: 480–489. [PubMed: 23915072]

66. Rimkus TK, Carpenter RL, Qasem S, Chan M, Lo HW. Targeting the Sonic Hedgehog Signaling Pathway: Review of Smoothened and GLI Inhibitors. Cancers 2016; 8.

67. Carpenter RL, Han W, Paw I, Lo HW. HER2 phosphorylates and destabilizes pro-apoptotic PUMA, leading to antagonized apoptosis in cancer cells. PLoS One 2013; 8: e78836. [PubMed: 24236056]

68. Carpenter RL, Lo HW. Regulation of Apoptosis by HER2 in Breast Cancer. Journal of carcinogenesis & mutagenesis 2013; 2013.

69. Hindley C, Philpott A. The cell cycle and pluripotency. Biochem J 2013; 451: 135–143. [PubMed: 23535166]

70. Kiuchi N, Nakajima K, Ichiba M, Fukada T, Narimatsu M, Mizuno K et al. STAT3 is required for the gp130-mediated full activation of the c-myc gene. The Journal of experimental medicine 1999; 189: 63–73. [PubMed: 9874564]

71. Foshay KM, Gallicano GI. Regulation of Sox2 by STAT3 initiates commitment to the neural precursor cell fate. Stem cells and development 2008; 17: 269–278. [PubMed: 18447642]

72. Okumura F, Okumura AJ, Matsumoto M, Nakayama KI, Hatakeyama S. TRIM8 regulates Nanog via Hsp90beta-mediated nuclear translocation of STAT3 in embryonic stem cells. Biochim Biophys Acta 2011; 1813: 1784–1792. [PubMed: 21689689]

73. Marotta LL, Almendro V, Marusyk A, Shipitsin M, Schemme J, Walker SR et al. The JAK2/STAT3 signaling pathway is required for growth of CD44(+)CD24(−) stem cell-like breast cancer cells in human tumors. J Clin Invest 2011; 121: 2723–2735. [PubMed: 21633165]

74. Snigdha K, Gangwani KS, Lapalikar GV, Singh A, Kango-Singh M. Hippo Signaling in Cancer: Lessons From Drosophila Models. Frontiers in Cell and Developmental Biology (Review) 2019; 7.

75. Hsu T-H, Yang C-Y, Yeh T-H, Huang Y-C, Wang T-W, Yu J-Y. The Hippo pathway acts downstream of the Hedgehog signaling to regulate follicle stem cell maintenance in the Drosophila ovary. Scientific Reports 2017; 7: 4480. [PubMed: 28667262]

76. Fernandez-L A, Northcott PA, Dalton J, Fraga C, Ellison D, Angers S et al. YAP1 is amplified and up-regulated in hedgehog-associated medulloblastomas and mediates Sonic hedgehog-driven neural precursor proliferation. Genes & development 2009; 23: 2729–2741. [PubMed: 19952108]

77. Zhu C, Li L, Zhao B. The regulation and function of YAP transcription co-activator. Acta Biochimica et Biophysica Sinica 2014; 47: 16–28. [PubMed: 25487920]

78. Ramos A, Camargo FD. The Hippo signaling pathway and stem cell biology. Trends in cell biology 2012; 22: 339–346. [PubMed: 22658639]

79. Gruber R, Panayiotou R, Nye E, Spencer-Dene B, Stamp G, Behrens A. YAP1 and TAZ Control Pancreatic Cancer Initiation in Mice by Direct Up-regulation of JAK-STAT3 Signaling. Gastroenterology 2016; 151: 526–539. [PubMed: 27215660]
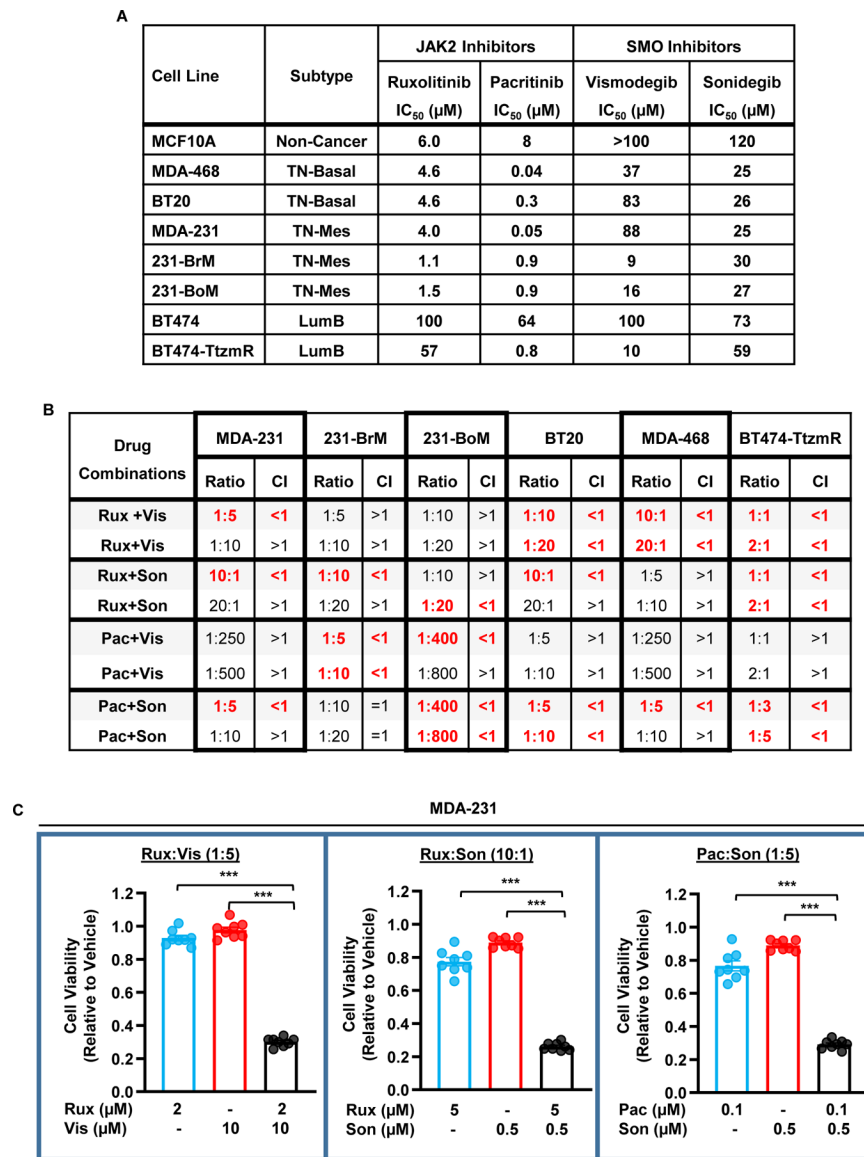
80. Overholtzer M, Zhang J, Smolen GA, Muir B, Li W, Sgroi DC et al. Transforming properties of YAP, a candidate oncogene on the chromosome 11q22 amplicon. Proceedings of the National Academy of Sciences of the United States of America 2006; 103: 12405–12410. [PubMed: 16894141]

A

Cell Line	Subtype	JAK2 Inhibitors		SMO Inhibitors	
		Ruxolitinib IC$_{50}$ (µM)	Pacritinib IC$_{50}$ (µM)	Vismodegib IC$_{50}$ (µM)	Sonidegib IC$_{50}$ (µM)
MCF10A	Non-Cancer	6.0	8	>100	120
MDA-468	TN-Basal	4.6	0.04	37	25
BT20	TN-Basal	4.6	0.3	83	26
MDA-231	TN-Mes	4.0	0.05	88	25
231-BrM	TN-Mes	1.1	0.9	9	30
231-BoM	TN-Mes	1.5	0.9	16	27
BT474	LumB	100	64	100	73
BT474-TtzmR	LumB	57	0.8	10	59

B

Drug Combinations	MDA-231		231-BrM		231-BoM		BT20		MDA-468		BT474-TtzmR	
	Ratio	CI	Ratio	CI	Ratio	CI	Ratio	CI	Ratio	CI	Ratio	CI
Rux +Vis	1:5	<1	1:5	>1	1:10	>1	1:10	<1	10:1	<1	1:1	<1
Rux+Vis	1:10	>1	1:10	>1	1:20	>1	1:20	<1	20:1	<1	2:1	<1
Rux+Son	10:1	<1	1:10	<1	1:10	>1	10:1	<1	1:5	>1	1:1	<1
Rux+Son	20:1	>1	1:20	>1	1:20	<1	20:1	>1	1:10	>1	2:1	<1
Pac+Vis	1:250	>1	1:5	<1	1:400	<1	1:5	>1	1:250	>1	1:1	>1
Pac+Vis	1:500	>1	1:10	<1	1:800	>1	1:10	>1	1:500	>1	2:1	>1
Pac+Son	1:5	<1	1:10	=1	1:400	<1	1:5	<1	1:5	<1	1:3	<1
Pac+Son	1:10	>1	1:20	=1	1:800	<1	1:10	<1	1:10	>1	1:5	<1

C

Figure 1: JAK2 and SMO inhibitors synergize to suppress TNBC and HER2-positive/ trastuzumab-resistant breast cancer *in vitro*.

(**A**) IC$_{50}$ values calculated from the results of the CellTiter Blue assay. Cell lines were seeded in 96-well plates and treated with test compound for 48 hours. (**B**) Combination Index (CI) values calculated for various drug combinations and ratios using CompuSyn. Breast cancer cells were seeded in 96-well plates and treated with drug combinations for 48 hours. Only a selection of tested drug ratios is shown. CI<1 indicates synergy, CI=1 indicates addition, and CI>1 indicates antagonism. Synergistic combinations are highlighted in red. (**C**) Normalized MDA-231 cell viability following combination treatments. Experiments were repeated at least three times to derive averages. Data are presented as mean ± SEM. One-way ANOVA with Tukey's multiple comparison *post hoc* test was used to compute p values. TN, triple-negative. CL, claudin-low. LumB, Luminal B. Rux, ruxolitinib. Pac, pacritinib. Vis, vismodegib. Son, sonidegib. TtzmR, trastuzumab-resistant. ***, $p < 0.001$.
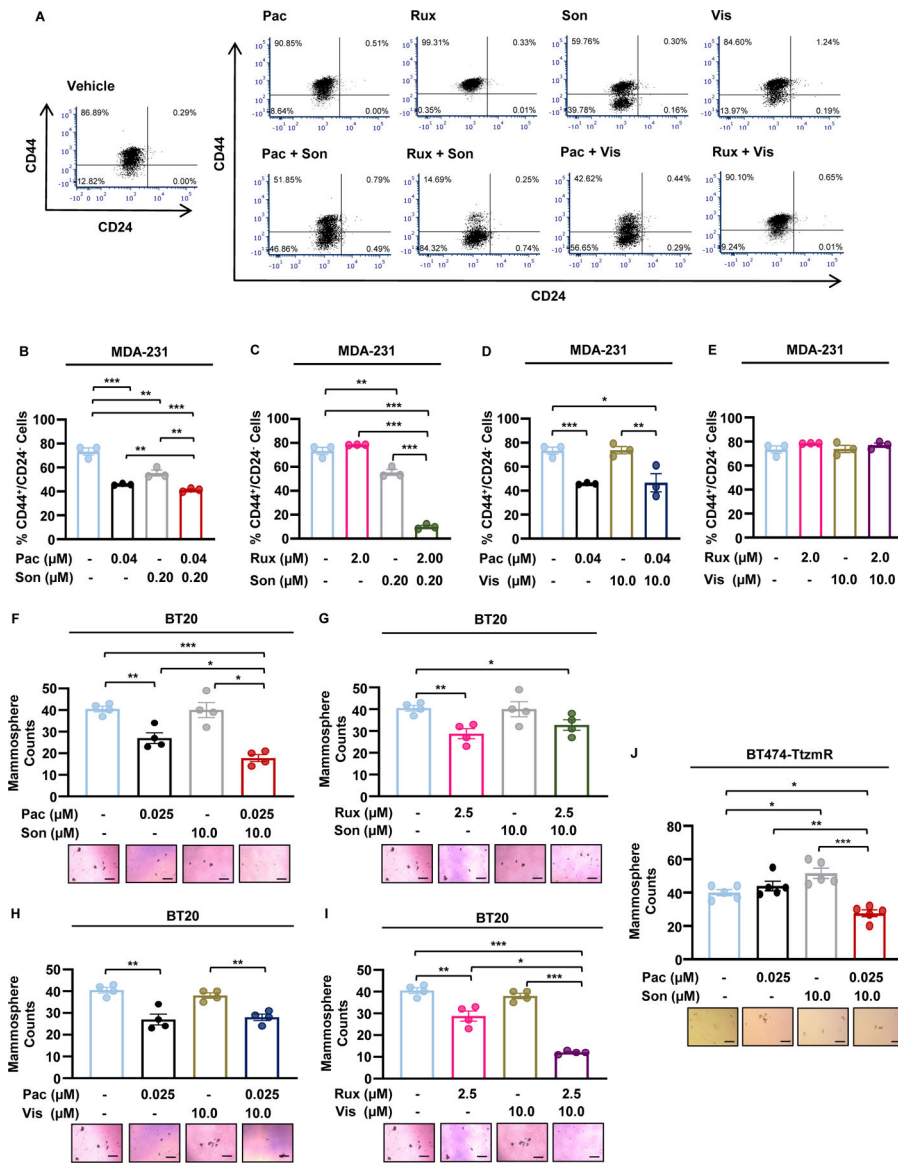
Figure 2: Simultaneous inhibition of JAK2-STAT3 and SMO signaling pathways suppress the cancer stem cell population.

(**A**) Representative flow cytometry scatter plots of CD44$^+$/CD24$^-$ MDA-231 cells. (**B–E**) Combination JAK2 inhibitor (JAK2i) and SMO inhibitor (SMOi) treatments more effectively suppressed the CD44^{high}/CD24^{low} MDA-231 population compared to single agent treatments alone as determined by FACS. The combinations of Pacritinib-Sonidegib (**B**) and Ruxolitinib-Soniedgib (**C**) were more effective than vehicle or either agent alone while the Pacritinib-Vismodegib (**D**) combination was not more effective than Pacritinib alone. The combination of Ruxolitinib-Vismodegib (**E**) did not suppress the CD44^{high}/CD24^{low} MDA-231 population. (**F-I**) Certain JAK2i-SMOi combination treatments synergized to more effectively inhibit BT20 mammosphere formation compared to single agent treatments alone. The combinations of Pacritinib-Sonidegib (**F**) and Ruxolitinib-Vismodegib (**I**) were more effective than vehicle or either agent alone while the Pacritinib-Vismodegib (**H**) combination was not more effective than Pacritinib alone. The combination

of Ruxolitinib-Sonidegib **(G)** did not inhibit mammosphere formation. **(J)** Pacritinib-Sonidegib combination treatment suppressed formation of BT474-TtzmR mammospheres. Representative BT20 or BT474-TtzmR mammosphere images are shown below the quantified data in each panel. Scale bars represent 200 μm. Data of three or four experimental repeats are presented as mean ± SEM. One-way ANOVA with Tukey's multiple comparison *post hoc* test was used to compute p values. *, $p < 0.05$; **, $p < 0.01$; ***, $p < 0.001$.
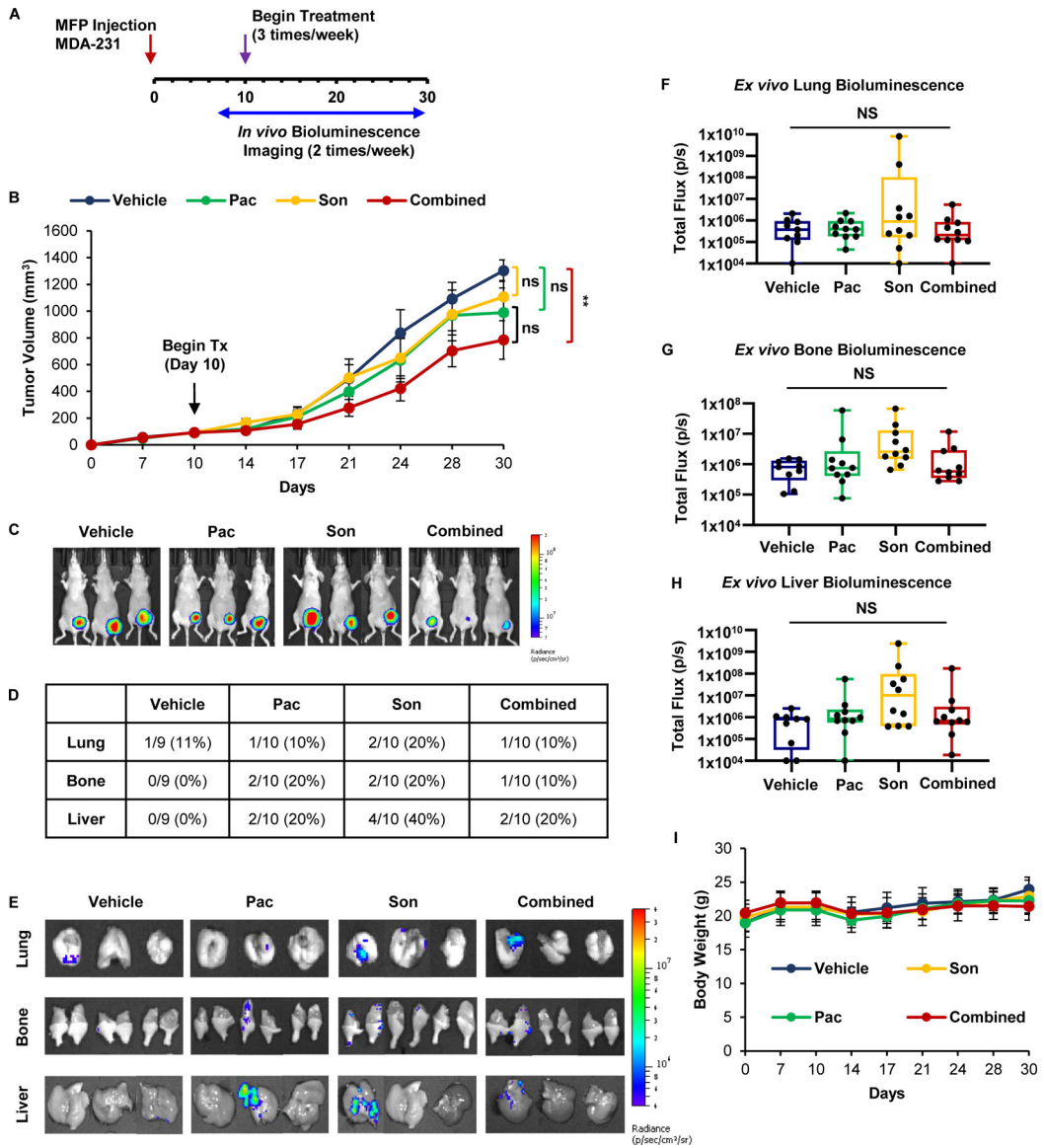
Figure 3: Co-treatment with JAK2 and SMO inhibitors suppresses the growth of TNBC tumors *in vivo*.

(**A**) Schema for MFP mouse model. Luciferase-expressing MDA-231 breast cancer cells were implanted into the left inguinal MFP. Tumor growth was assessed via caliper measurements and bioluminescent imaging. Once tumors reached an average of 90 mm^3, mice were randomized into vehicle, 7.5 mg/kg pacritinib, 20 mg/kg sonidegib, or combination treatment groups (N=9–10) and received three intraperitoneal treatments per week. (**B**) Growth curve for MFP tumors. (**C**) Representative bioluminescent images of xenograft-bearing female nude mice 30 days post-inoculation. (**D**) Quantification of organ-specific metastasis incidence. **E)** Representative bioluminescent *ex vivo* organ images are shown. (**F-H**) *Ex vivo* lung (**F**), bone (**G**), and liver (**H**) bioluminescence was quantified. (**I**) Average mouse weights over the course of the study. One-way ANOVA with Tukey's multiple comparison *post hoc* test was used to compute p values.
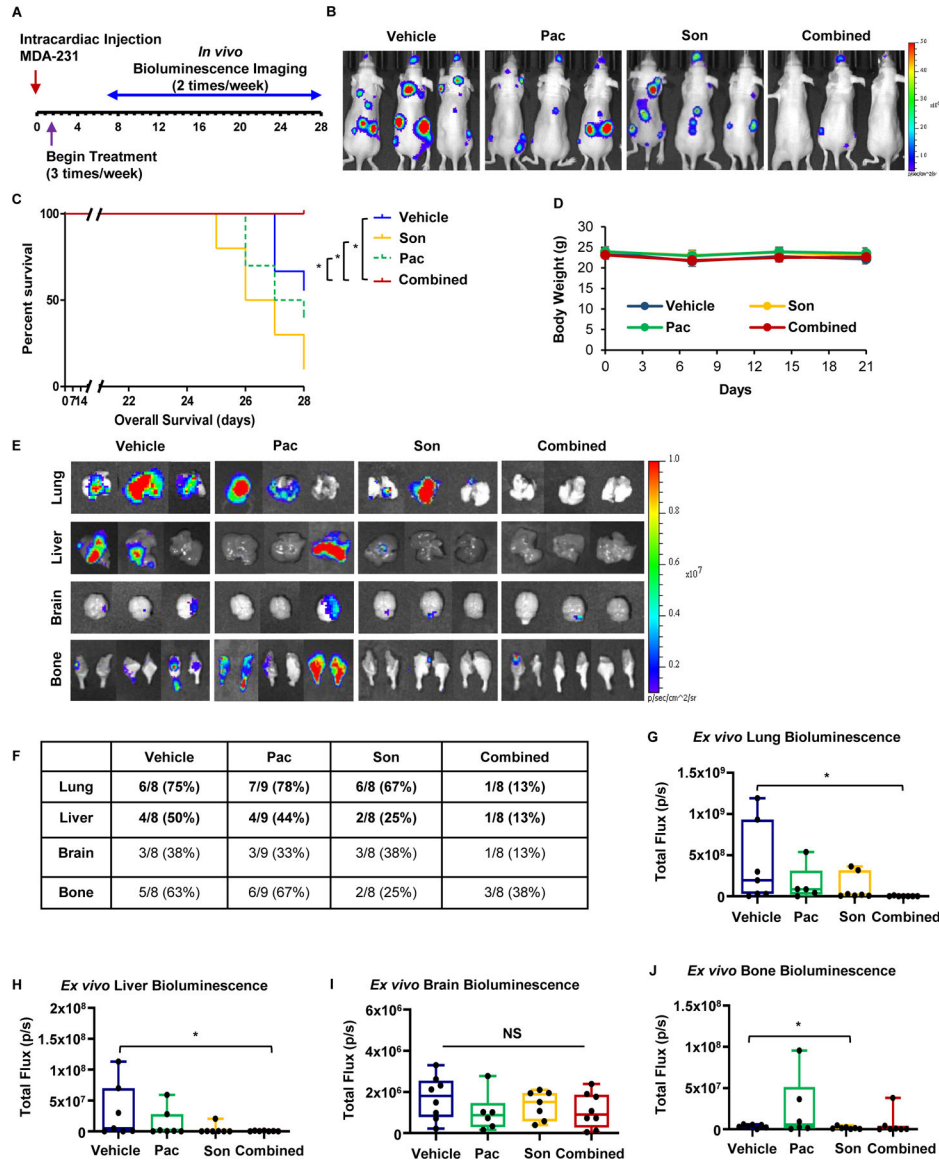
Figure 4: Combined treatment with JAK2 and SMO inhibitors synergistically reduced TNBC metastasis *in vivo*.

(A) Schema for intracardiac mouse model. Luciferase-expressing MDA-231 breast cancer cells were implanted intracardially via the left ventricle of female nude mice and tumor growth was assessed biweekly via bioluminescent imaging. Mice that underwent successful inoculations were randomized into vehicle, 7.5 mg/kg pacritinib, 20 mg/kg sonidegeib, or combination treatment groups (N=8–9) and received three intraperitoneal treatments per week. **(B)** Representative bioluminescent images of female nude mice 28 days post-inoculation. **(C)** Pacritinib-sondiegib combination treatment prolonged overall survival of mice bearing MDA-231 xenografts compared to vehicle or either agent alone. Mantel-Cox log-rank test was used to determine p values. **(D)** Average mouse weights over the course of the study. **(E)** Representative bioluminescent *ex vivo* organ images are shown. **(F)** Quantification of organ-specific metastasis incidence. **(G–J)** *Ex vivo* lung **(G)**, liver **(H)**,
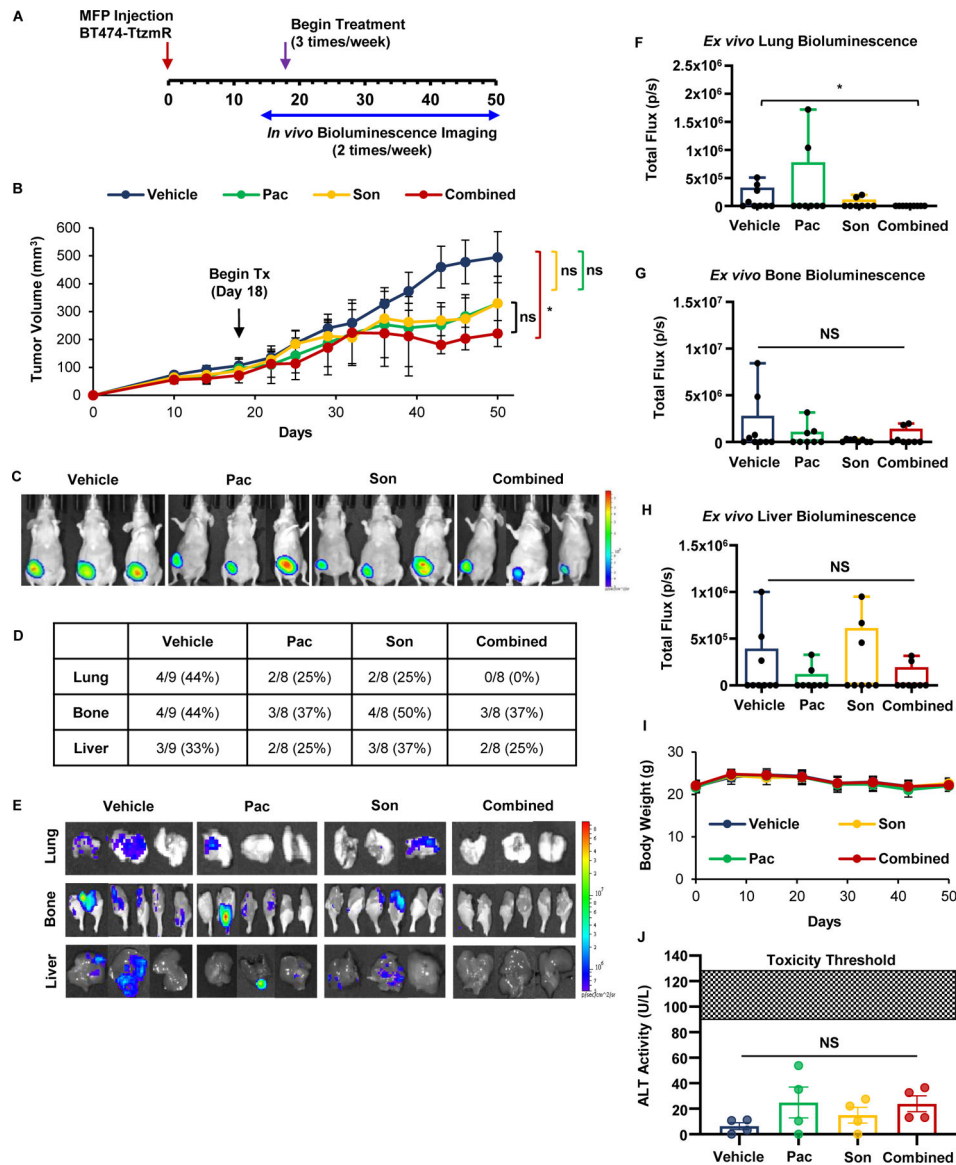
brain **(I)**, and **(J)** bone bioluminescence was quantified. One-way ANOVA with Tukey's multiple comparison *post hoc* test was used to compute p values. *, $p < 0.05$.

Figure 5: Co-treatment with JAK2 and SMO inhibitors suppresses the orthotopic growth and lung metastasis of HER2-positive/trastuzumab-resistant breast cancer *in vivo*.
(**A**) Schema for MFP mouse model. Luciferase-expressing BT474-TtzmR breast cancer cells were implanted into the right inguinal MFP. Tumor growth was assessed via caliper measurements and bioluminescent imaging. Once tumors reached an average of 90 mm³, mice were randomized into vehicle, 7.5 mg/kg pacritinib, 20 mg/kg sonidegib, or combination treatment groups (N=8–9) and received three intraperitoneal treatments per week. (**B**) Growth curve for MFP tumors. (**C**) Representative bioluminescent images of xenograft-bearing female nude mice 50 days post-inoculation. (**D**) Quantification of organ-specific metastasis incidence. (**E**) Representative bioluminescent *ex vivo* organ images are shown. (**F–H**) *Ex vivo* lung (**F**), bone (**G**), and liver (**H**) bioluminescence was quantified. (**I**) Average mouse weights over the course of the study. (**J**) Circulating alanine transaminase (ALT) levels were not significantly increased in any treatment group. Data presented as
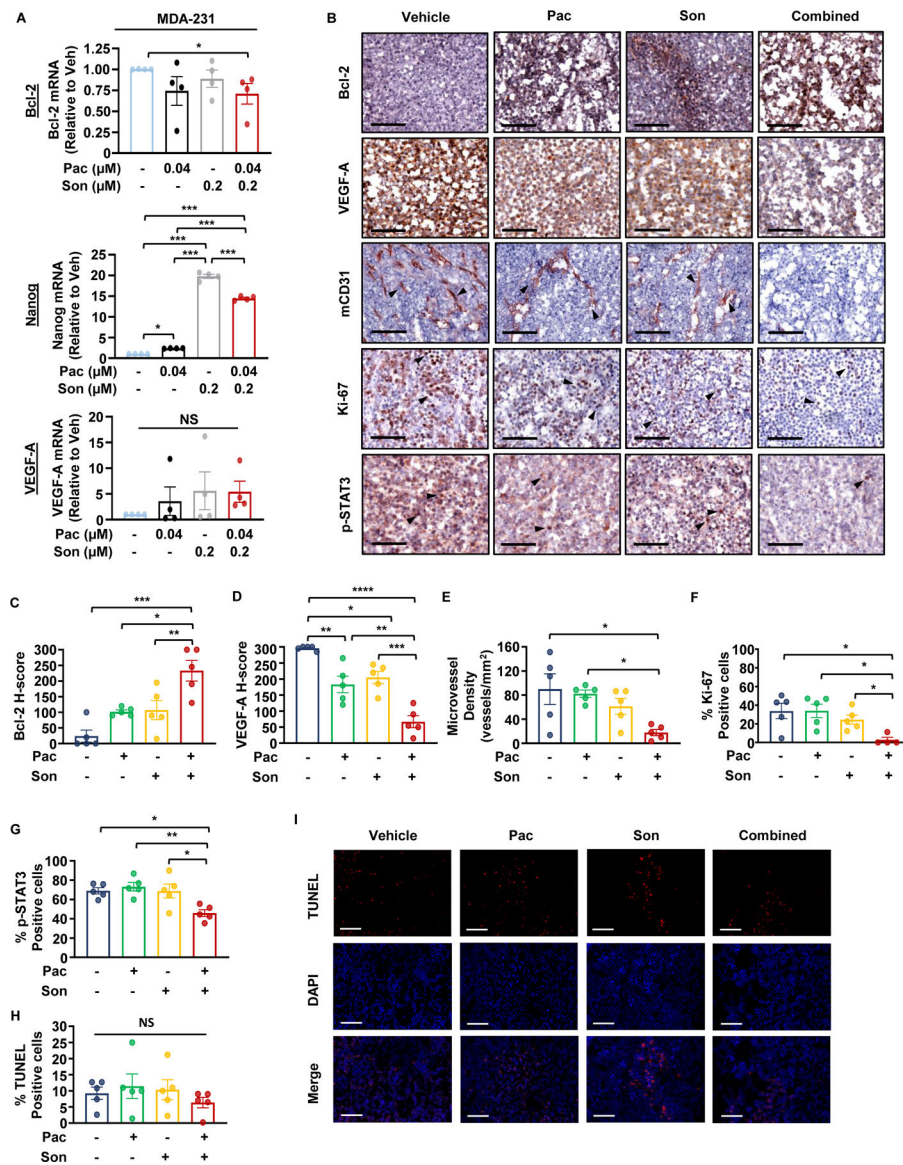
mean ± SEM. One-way ANVOA with Tukey's multiple comparison *post hoc* test was used to compute p values. *, p < 0.05

Figure 6: Combined treatment with JAK2 and SMO inhibitors synergize to reduce angiogenesis, tumor cell proliferation, and tumoral STAT3 activation of TNBC *in vivo*.

(A) RT-qPCR analysis of JAK2-STAT3 and SMO-GLI1/tGLI1 target genes following treatment of MDA-231 cells *in vitro*. **(B)** Representative IHC images of Bcl-2, VEGF-A, mCD31, Ki-67, and p-STAT3 (Y705) of treated MDA-231 MFP xenografts. Images were taken under 20X magnification. Arrows point to examples of positive staining. **(C–G)** Quantification histologic staining of Bcl-2 **(C)**, VEGF-A **(D)**, mCD31 (microvessel density; **(E)**, % Ki-67 positivity **(F)**, and % p-STAT3 (Y705) positivity **(G)** of MDA-231 mammary fat pad xenografts. **(H)** Quantification of the number of TUNEL positive cells of mammary fat pad xenografts from each treatment group. **(I)** Representative images of TUNEL-positive staining of mammary fat pad xenografts from each treatment group. TUNEL, DAPI, and TUNEL-DAPI merged. Images were taken under 10X magnification. For all analyses, at least 5 fields were quantified per tumor section (N=3–4 tumors/group). All scale bars represent 100 μm. Data presented as mean ± SEM. One-way ANOVA with Tukey's multiple

comparison *post hoc* test was used to compute p values. *, $p < 0.05$; **, $p < 0.01$; ***, $p < 0.001$; ****, $p < 0.0001$.

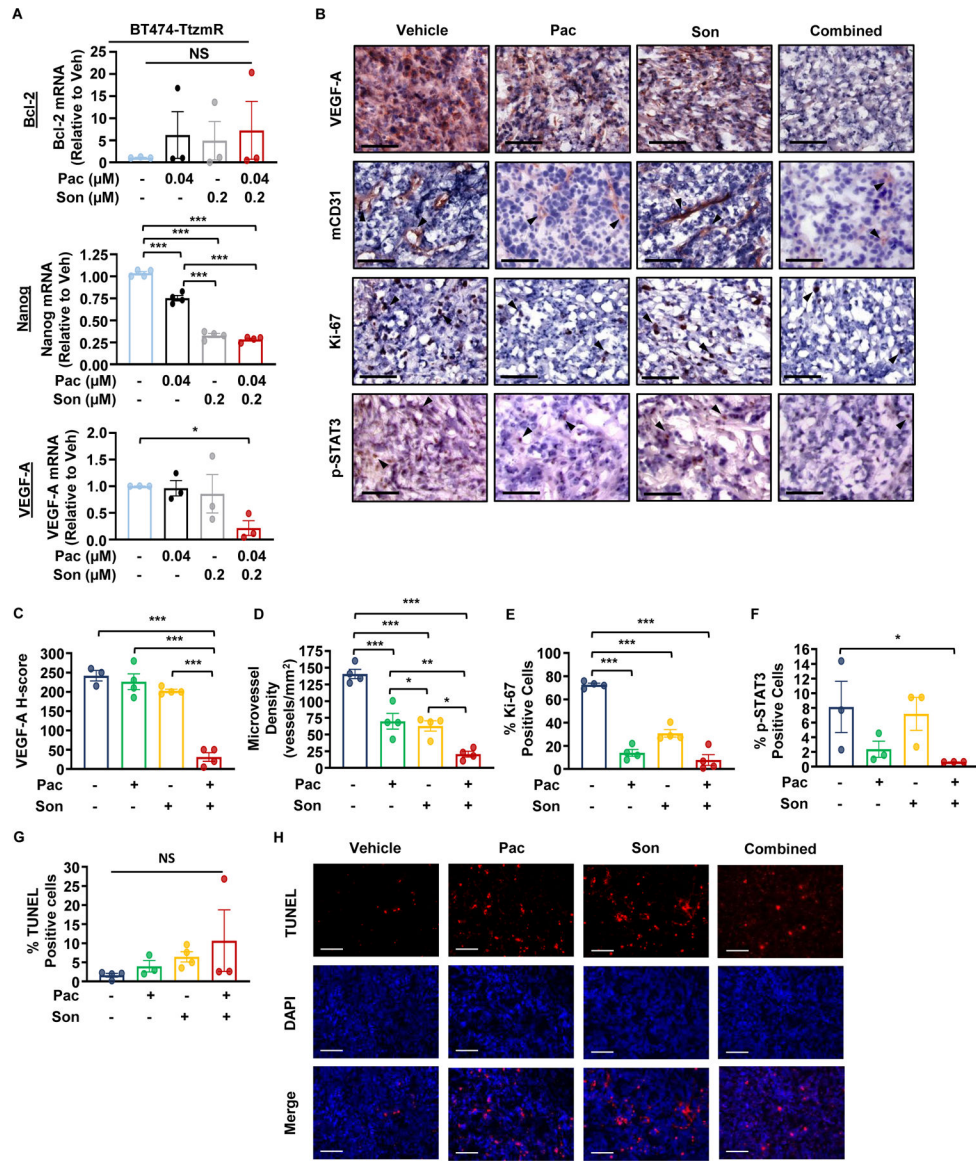**Figure 7: JAK2 and SMO inhibitors synergize to reduce angiogenesis, tumor cell proliferation, and STAT3 activation of HER2-positive, trastuzumab-resistant breast cancer *in vivo*.**

(A) RT-qPCR analysis of JAK2-STAT3 and SMO-GLI1/tGLI1 target genes following treatment of BT474-TtzmR cells *in vitro*. **(B)** Representative IHC images of VEGF-A, mCD31, Ki-67, and p-STAT3 (Y705) of treated BT474-TtzmR mammary fat pad xenografts. Images were taken under 20X magnification. Arrows point to examples of positive staining. **(C–E)** Quantification of histologic staining of VEGF-A **(C)**, mCD31 (microvessel density; **(D)**, % Ki-67 positivity **(E)**, and % p-STAT3 (Y705) positivity **(F)** of treated BT474-TtzmR MFP xenografts. **(G)** Quantification of the number of TUNEL positive cells of mammary fat pad xenografts from each treatment group. **(H)** Representative images of TUNEL-positive staining of mammary fat pad xenografts from each treatment group. TUNEL, DAPI, and TUNEL-DAPI merged. Images were taken under 10X magnification. For all analyses, at least 5 fields were quantified per tumor section (N=4–5 tumors/group). All scale bars represent 100 µm. Pac, pacritinib. Son, sonidegib. Data presented as mean ± SEM. One-way

ANOVA with Tukey's multiple comparison *post hoc* test was used to compute p values. *, p < 0.05; **, p < 0.01; ***, p < 0.001.